Modeling of Wave Propagation in Unbounded Domains Using the Scaled Boundary Finite Element Method

***Xiaojun Chen, Carolin Birk, Chongmin Song**

School of Civil and Environmental Engineering, University of New South Wales, Australia.

*Corresponding author: xiaojun.chen@unsw.edu.au

Abstract

In this paper the dynamic soil-structure interaction problem is modeled using a scaled boundary finite element method (SBFEM) in the time domain. The original SBFEM formulation assumes a piece-wise constant approximation of the acceleration unit-impulse response matrix within one time step. A small maximum step size is required to make the algorithm stable. In this paper, the procedure is formulated in terms of the displacement unit-impulse response matrix, which leads two essential improvements: (1) the displacement unit-impulse response matrix is calculated using a more accurate and efficient approach, based on a piece-wise linear approximation; (2) the soil-structure interaction force described by the convolution integral is only calculated before a truncation time, which reduces the computational effort. Derivations of the corresponding efficient schemes will be presented and verified using numerical examples.

Keywords: dynamic soil-structure interaction, wave propagation, time domain, scaled boundary finite element method, displacement unit-impulse response matrix

1. Introduction

The numerical modeling of wave propagation in unbounded domains is required in a number of engineering applications, such as soil-structure interaction analysis or dam-reservoir interaction analysis. Here, the well-established finite element method cannot be used straightforwardly, since outgoing waves are reflected at the artificial boundaries of the finite element mesh, such that special measures have to be taken to prevent these reflections (Givoli, 1999), (Tsynkov, 1998). A popular method for the analysis of dynamic problems in unbounded media is the boundary element method, because the radiation condition is fulfilled explicitly by the fundamental solution (Beskos, 1987), (Beskos, 1997). The idea of extending the finite element mesh towards infinity has driven the development of infinite element techniques (Bettess, 1992). A recent technique, which is particularly suitable for modeling time-dependent problems in infinite media, is the scaled boundary finite element method (SBFEM) (Wolf & Song, 1997). This semi-analytical technique is based on a combination of a numerical solution in the circumferential directions with an analytical solution in the direction of wave propagation. Thus, radiation damping is modeled accurately.

The structure (near field) can be modeled by either conventional finite element method or scaled boundary finite element method. The soil (far field) is modeled by scaled boundary finite element method. As shown in Figure 1, the connection between the near field and far field can be expressed in terms of the displacement vector $\{u\}$ and the force vector $\{R\}$. In the frequency domain, the force displacement relationship is

$$\{R(\omega)\} = [S^{\infty}(\omega)]\{u(\omega)\}, \tag{1}$$

where $[S^{\infty}(\omega)]$ is the dynamic stiffness matrix. In SBFEM, it can be calculated by (Wolf & Song, 1997),

$$([S^{\infty}(\omega)] + [E^1])[E^0]^{-1}([S^{\infty}(\omega)] + [E^1]^T) - (s-2)[S^{\infty}(\omega)] - \omega[S^{\infty}(\omega)]_{,\omega} - [E^2] - \omega[M^0] = 0, \quad (2)$$

where $[E^0]$, $[E^1]$, $[E^2]$ and $[M^0]$ are the SBFE coefficient matrices and $s = (2 \text{ or } 3)$ is the spatial dimension (Wolf & Song, 1997), Equation (2) is called the SBFE equation in dynamic stiffness matrix.

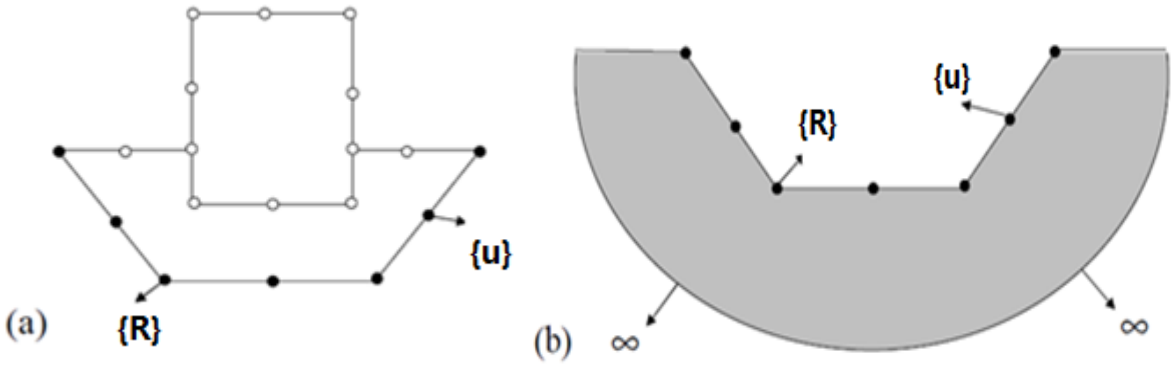

Figure 1. (a) Structure (near field); (b) Soil (far field).

In order to obtain the force-displacement relationship in the time domain, inverse Fourier transform needs to be applied to Equations (1) and (2). As $[S^{\infty}(\omega)]$ is not square integrable, it contains a singular part $[S_s^{\infty}(\omega)]$ and a regular part $[S_r^{\infty}(\omega)]$. In order to avoid numerical singularity, Equation (2) is alternatively expressed in terms of the acceleration dynamic stiffness matrix $[M^{\infty}(\omega)] = [S^{\infty}(\omega)]/(i\omega)^2$ in the original SBFEM. This results in the force-acceleration relationship in the time domain,

$$\{R(t)\} = \int_0^t [M^{\infty}(\tau)]\{\ddot{u}(t-\tau)\}d\tau, \quad (3)$$

where $[M^{\infty}(t)]$ is the acceleration unit-impulse response matrix, which is determined by

$$\int_0^t [m^{\infty}(t-\tau)][m^{\infty}(\tau)]d\tau + t\int_0^t [m^{\infty}(\tau)]d\tau + [e^1]\int_0^t\int_0^{\tau} [m^{\infty}(\bar{\tau})]d\bar{\tau}d\tau + \int_0^t\int_0^{\tau} [m^{\infty}(\bar{\tau})]d\bar{\tau}d\tau\,[e^1]^T - \frac{t^3}{6}[e^2]H(t) - t[m^0]H(t) = 0, \quad (4)$$

which is the transformed form of the equation for the acceleration unit-impulse response matrix (Wolf & Song, 1997). Equation (4) has to be solved by time discretization. The original time discretization scheme is based on a piece-wise constant variation of $[m^{\infty}(t)]$, and the time step size need to be set very small in order to keep the numerical results stable. Recently, a new time discretization scheme has been proposed by assuming $[m^{\infty}(t)]$ to be piece-wise linear, and

introducing an extrapolation parameter θ. This leads to improved stability and allows a larger time step size to be used (Radmanovic & Katz, 2010).

As $[S_r^\infty(t)]$ converges to zero for later time, it is worthwhile to obtain an equation similar to Equation (4) for $[S_r^\infty(t)]$, and to employ a new similar time discretization scheme. In the time domain analysis, a truncation time can be introduced to reduce the total computational cost.

The objective of this paper is to first derive the SBFE equation for the displacement unit-impulse response matrix and propose the corresponding time discretization scheme. Then the time domain formulation is established while introducing the truncation at the same time.

The further outline of this paper is as follows. In Section 2, the SBFE equation for the displacement unit-impulse response matrix is derived and its time discretization scheme is proposed. The stability and efficiency of the method are investigated. In Section 3, algorithms for the interface force-displacement relationship are developed. In Section 4, numerical example is used to evaluate the new scheme. Concluding remarks are stated in Section 5.

2. SBFE equation for displacement unit-impulse response matrix

In this section a new numerical scheme for the computation of the displacement unit-impulse response matrix is derived. It starts from the transformed SBFE equation in dynamic stiffness $[s^\infty(\omega)]$ in the frequency domain (Wolf & Song, 1997), which is given as:

$$\begin{aligned}([s^\infty(\omega)]+[e^1])([s^\infty(\omega)]+[e^1]^T)-(s-2)[s^\infty(\omega)]-\omega[s^\infty(\omega)]_{,\omega}-[e^2]\\ -(i\omega)^2\lceil\Lambda^2\rfloor=0.\end{aligned} \tag{5}$$

Equation (5) is obtained by performing the following eigenvalue decomposition:

$$[M^0][\Phi]=[E^0][\Phi]\lceil\Lambda^2\rfloor. \tag{6}$$

Details can be found in (Wolf & Song, 1998).Then, $[s^\infty(\omega)]$ is decomposed as

$$[s^\infty(\omega)]=i\omega[c_\infty]+[k_\infty]+\frac{1}{i\omega}[a_1]+[s_r^*(\omega)], \tag{7}$$

where the first two terms comprise the singular part $[s_s^\infty(\omega)]$. $[c_\infty]$ is the transformed dashpot matrix and $[k_\infty]$ is the transformed spring matrix. The last two terms in Equation (7) comprise the regular part

$$[s_r^\infty(\omega)]=\frac{1}{i\omega}[a_1]+[s_r^*(\omega)]. \tag{8}$$

Substituting Equation (7) into Equation (5) leads to a polynomial in $(i\omega)$. Individual terms corresponding to different powers of $(i\omega)$ must be equal to zero. The terms corresponding to $(i\omega)^2$, $(i\omega)^1$ and $(i\omega)^0$ are used to calculate $[c_\infty]$, $[k_\infty]$ and $[a_1]$ (Wolf J. , 2003). Setting the remaining terms equal to zero yields an equation for $[s_r^*(\omega)]$,

$$
\begin{aligned}
&[s_r^*(\omega)][s_r^*(\omega)] \\
&+ [a_1]\frac{[s_r^*(\omega)]}{i\omega} + \frac{[s_r^*(\omega)]}{i\omega}[a_1] + ([k_\infty] + [e^1])[s_r^*(\omega)] + [s_r^*(\omega)]([k_\infty] + [e^1]^{\mathrm{T}}) \\
&\quad + [c_\infty](i\omega[s_r^*(\omega)]) + (i\omega[s_r^*(\omega)])[c_\infty] \\
&\quad + \frac{1}{i\omega}\Big(([k_\infty] + [e^1])[a_1] + [a_1]([k_\infty] + [e^1]^{\mathrm{T}})\Big) + \frac{1}{(i\omega)^2}[a_1]^2 \\
&\quad - (s-3)\frac{1}{i\omega}[a_1] - (s-2)[s_r^*(\omega)] - \omega[s_r^*(\omega)]_{,\omega} = 0,
\end{aligned}
\tag{9}
$$

Applying the inverse Fourier transform to Equation (9) yields:

$$
\begin{aligned}
&\int_0^t [s_r^*(t-\tau)][s_r^*(\tau)]d\tau + [a_1]\left(\int_0^t [s_r^*(\tau)]\,d\tau\right) + \left(\int_0^t [s_r^*(\tau)]\,d\tau\right)[a_1] \\
&\quad + ([k_\infty] + [e^1])[s_r^*(t)] + [s_r^*(t)]([k_\infty] + [e^1]^T) + [c_\infty]\frac{d[s_r^*(t)]}{dt} \\
&\quad + \frac{d[s_r^*(t)]}{dt}[c_\infty] + t\frac{d[s_r^*(t)]}{dt} - (s-3)[s_r^*(t)] \\
&\quad + ([k_\infty][a_1] + [a_1][k_\infty] + [a_1][e^1]^T + [e^1][a_1] - (s-3)[a_1])H(t) \\
&\quad + t[a_1]^2 H(t) = 0,
\end{aligned}
\tag{10}
$$

Also applying the inverse Fourier transform to Equation (8) yields

$$
[s_r^\infty(t)] = [a_1] + [s_r^*(t)], \qquad \text{for } t \geq 0 \tag{11}
$$

Substituting Equation (11) into Equation (10) yields

$$
\begin{aligned}
&\int_0^t [s_r^\infty(t-\tau)][s_r^\infty(\tau)]d\tau + ([k_\infty] + [e^1])[s_r^\infty(t)] + [s_r^\infty(t)]([k_\infty] + [e^1]^T) + [c_\infty]\frac{d[s_r^\infty(t)]}{dt} \\
&\quad + \frac{d[s_r^\infty(t)]}{dt}[c_\infty] + t\frac{d[s_r^\infty(t)]}{dt} - (s-3)[s_r^\infty(t)] = 0,
\end{aligned}
\tag{12}
$$

Equation (12) is a first order ordinary differential equation with a convolution integral, with initial value (Wolf & Song, 1997)

$$
[s_r^\infty(t=0)] = [a_1], \tag{13}
$$

Generally, there is no analytical solution for Equation (12), so it needs to be solved by time discretization scheme, i.e. the total time history is discretized into a number of time steps $t = t_n = n\Delta t$, where Δt is the time step size. So the whole time history is divided into n time intervals: $[(i-1)\Delta t,\ i\Delta t]\ \ (i = 1,2,\dots,n)$. It is assumed, that $[\dot{s}_r^\infty(t)] = \frac{d[s_r^\infty(t)]}{dt}$ changes linearly within each time interval. At each time step $t_i = i\Delta t$, the following procedures are used:

a) An extrapolation parameter $\theta \in [1,2]$ is introduced. Equation (12) is evaluated at time $t = (i-1+\theta)\Delta t$. The convolution integral in Equation (12) is discretized into $i-1$

intervals of length Δt and one final interval of length $\theta\Delta t$. Within that extended interval $[\dot{s}_r^{\infty}(t)]$ is assumed to vary linearly.

b) The corresponding$[s_r^{\infty}(t)]$ within the interval $[(i-1)\Delta t,\ (i-1+\theta)\Delta t]$ has the following expression,

$$[s_r^{\infty}(t)] = [s_r^{\infty}]_{i-1+\theta} = [s_r^{\infty}]_{i-1} + \tau[\dot{s}_r^{\infty}]_{i-1} + \frac{\tau^2}{2\theta\Delta t}([\dot{s}_r^{\infty}]_{i-1+\theta} - [\dot{s}_r^{\infty}]_{i-1}), \tag{14}$$

where $[s_r^{\infty}]_{i-1}$ is the value of $[s_r^{\infty}(t)]$ at $t=(i-1)\Delta t$, $[\dot{s}_r^{\infty}]_{i-1}$ and $[\dot{s}_r^{\infty}]_{i-1+\theta}$ are the value of $[\dot{s}_r^{\infty}(t)]$ at $t=(i-1)\Delta t$ and $t=(i-1+\theta)\Delta t$, respectively. τ is the local coordinate $\tau = t-(i-1)\Delta t$;

c) The discretized formulation of Equation (12) is solved for $[\dot{s}_r^{\infty}]_{i-1+\theta}$. Then $[s_r^{\infty}(t=i\Delta t)]$ is determined using,

$$[s_r^{\infty}(t=i\Delta t)] = [s_r^{\infty}]_i = [s_r^{\infty}]_{i-1} + \Delta t[\dot{s}_r^{\infty}]_{i-1} + \frac{\Delta t}{2\theta}([\dot{s}_r^{\infty}]_{i-1+\theta} - [\dot{s}_r^{\infty}]_{i-1}). \tag{15}$$

Steps (a) – (c) are repeated for each time step $[s_r^{\infty}]_i$ $(i=1,2,\dots,n)$. Finally the displacement unit-impulse response matrix $[S_r^{\infty}(t)]$ is calculated as,

$$[S_r^{\infty}(t=i\Delta t)] = [\Phi]^{-T}[s_r^{\infty}]_i[\Phi]^{-1}. \tag{16}$$

In order to verify the stability of this algorithm, a two-dimensional example of a rigid strip foundation is analyzed (Figure 2). The displacement unit-impulse response matrix is calculated using the proposed method, and compared to the original constant scheme (Wolf & Song, 1998). In order to make the results comparable, a rigid vertical motion pattern $\{\varphi\}$ is enforced on the displacement unit-impulse response, i.e. ${S^{\infty}}_{vv}(t) = \{\varphi\}^T[S_r^{\infty}(t)]\{\varphi\}$. ${S^{\infty}}_{vv}(t)$ is then normalized by the factor $b/(Gc_s)$ and plotted in Figure 3.

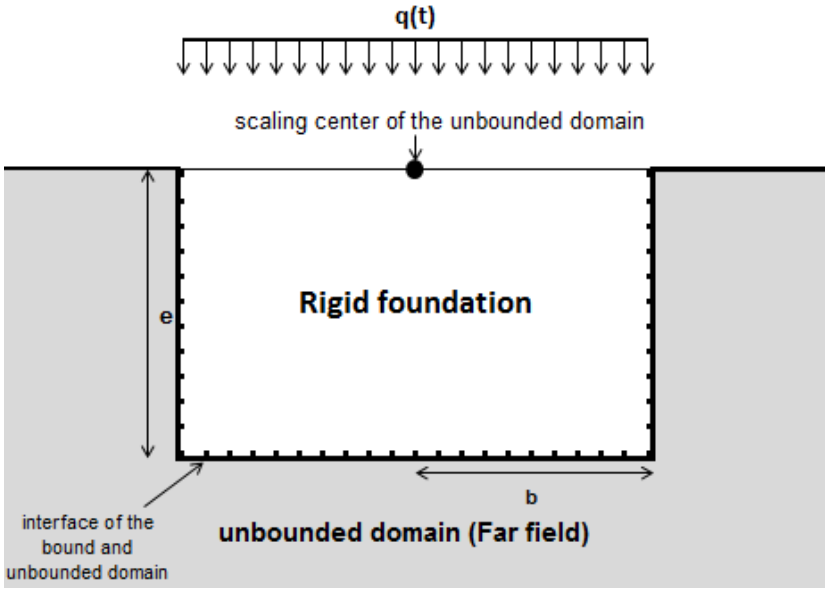

Figure 2. Two-dimensional rigid strip foundation embedded in isotropic and homogeneous half-space

It can be noted, that the original scheme (const) is stable for relatively small dimensionless time step size $\Delta t' = \Delta t c_s / b = 0.02$. For dimensionless time step size $\Delta t' = 0.05$, it becomes unstable very early, while for the proposed method with $\theta = 1.8$, the result is stable. Even if we choose large time step size $\Delta t' = 0.2$, no oscillation occurs in the solution. This example shows that the algorithm for the displacement unit-impulse response matrix can be used for larger time steps.

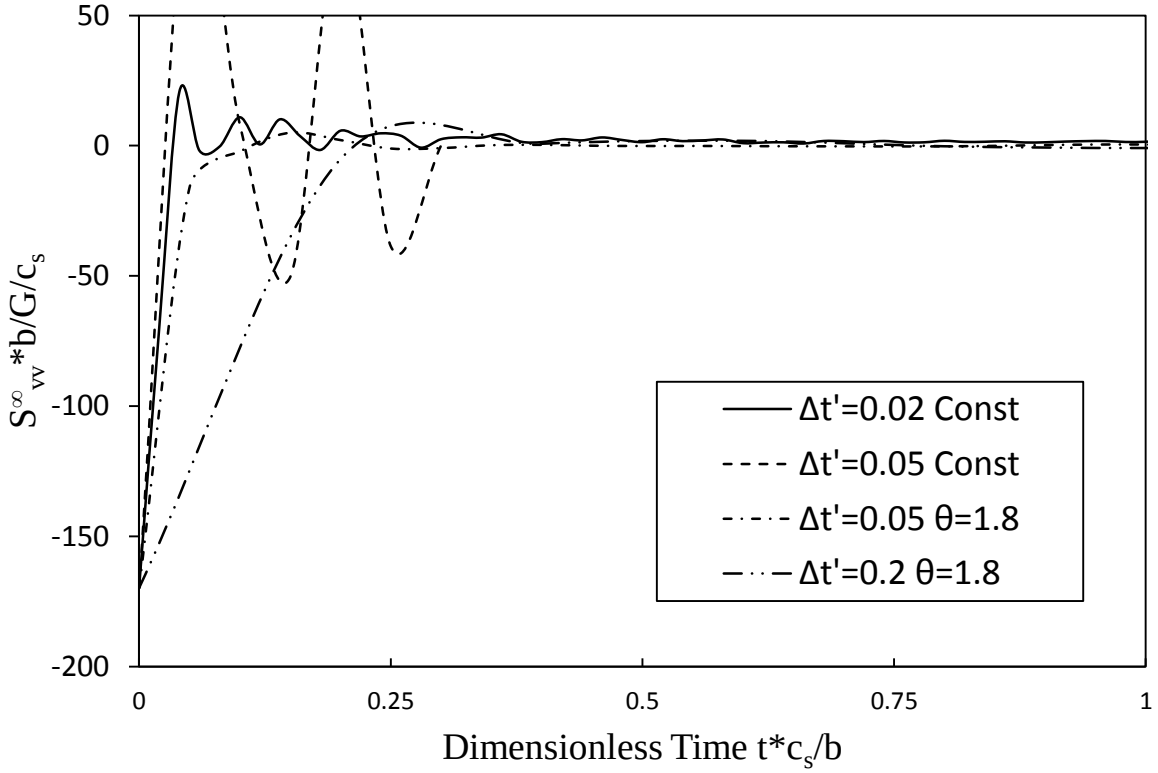

Figure 3. Comparison of the stability of the normalized unit-impulse response coefficient of the rigid foundation

3. Integration of the soil-structure interaction force

The soil-structure interaction force vector $\{R(t)\}$ is given by the convolution integral (Wolf & Song, 1997)

$$\{R(t)\} = [C_\infty]\{\dot{u}(t)\} + [K_\infty]\{u(t)\} + \int_0^t [S_r^\infty(\tau)]\{u(t-\tau)\}d\tau, \tag{17}$$

where $[C_\infty]$ and $[K_\infty]$ are the constant dashpot and spring matrix, respectively, while can be calculated in advance. The displacement unit-impulse response matrix $[S_r^\infty(t)]$ is given at discrete times: $t_i = i\Delta t, (i = 0,1, \dots, n)$. The discretization size for $\{u(t)\}$, however, is controlled by the frequency range of the input loading, and normally smaller than the time step size for $[S_r^\infty(t)]$. Therefore, linear interpolation of $[S_r^\infty(t)]$ is used to find intermediate values required to fit the smaller discretization size for $\{u(t)\}$. Thus, various time discretization schemes can be used to solve Equation (17), for example, the classical Newmark method.

In addition, as $[S_r^{\infty}(t)]$ converges to zero at later time, a truncation time $T = N\Delta t$ is introduced, i.e. $[S_r^{\infty}(t)] = 0$ for $t \geq T$. Thus Equation (17) can be reformulated as,

$$\{R(t)\} = [C_{\infty}]\{\dot{u}(t)\} + [K_{\infty}]\{u(t)\} + \int_0^T [S_r^{\infty}(\tau)]\{u(t-\tau)\}d\tau, \tag{18}$$

Therefore, after the truncation time T, the size of the convolution does not increase anymore and the computational cost is reduced. In the next section, a numerical example is used to demonstrate the efficiency of the method.

4. Numerical example

A flexible rectangular strip foundation embedded in homogeneous isotropic half-space, together with a deep trench next to the foundation is modeled (Figure 4). A uniformly distributed triangular pulse is applied on the surface of the foundation (Figure 5).

The near field includes the foundation and adjacent soil, and is divided into seven subdomains, which are modeled using the SBFEM described in (Song, 2009). The embedment ratio is $e/b = 1$ and three-node line elements are used, whose length uniformly equals $0.1b$. The scaling center of the subdomains in the near field is located at the center of the rectangle, except for subdomain 5 and 6, whose scaling center is located at the corner of the trench, in order to avoid stress concentration. The far field is modeled with one unbounded subdomain, whose scaling center is located at the top center of the near field (shown in Figure 4). For the near field, each subdomain is modeled with continued fraction and the order of the continued fraction is 2 (Song, 2009), yields the total number of degree of freedom to be 1756. The foundation has a shear modulus $G = 7GPa$, mass density $\rho = 2500kg/m^3$ and Poisson's ratio $\nu = 0.2$, while for the soil, $G = 0.125GPa$, $\rho = 2300kg/m^3$ and $\nu = 0.3$.

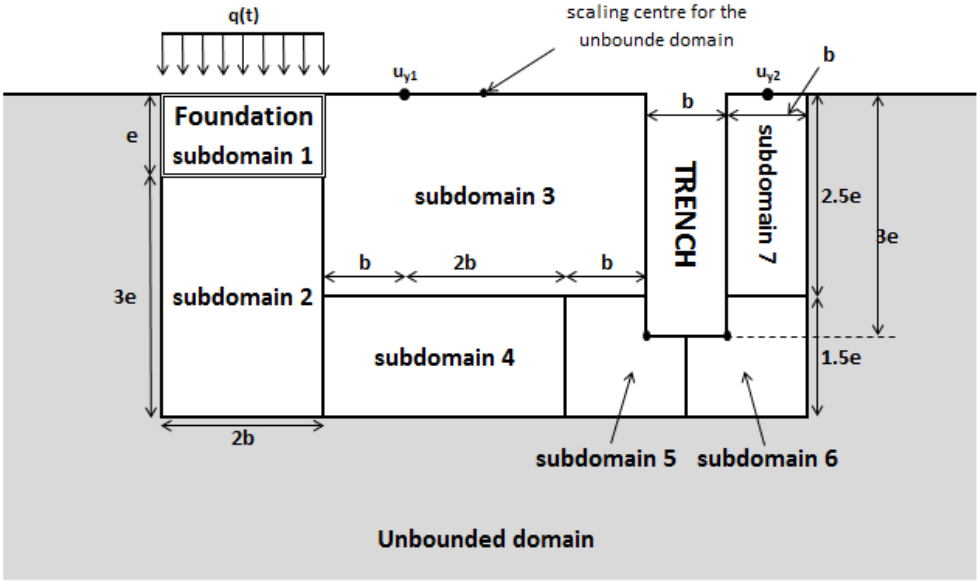

Figure 4. Illustration of the flexible foundation embedded in isotropic and homogeneous half-space with a trench next to it

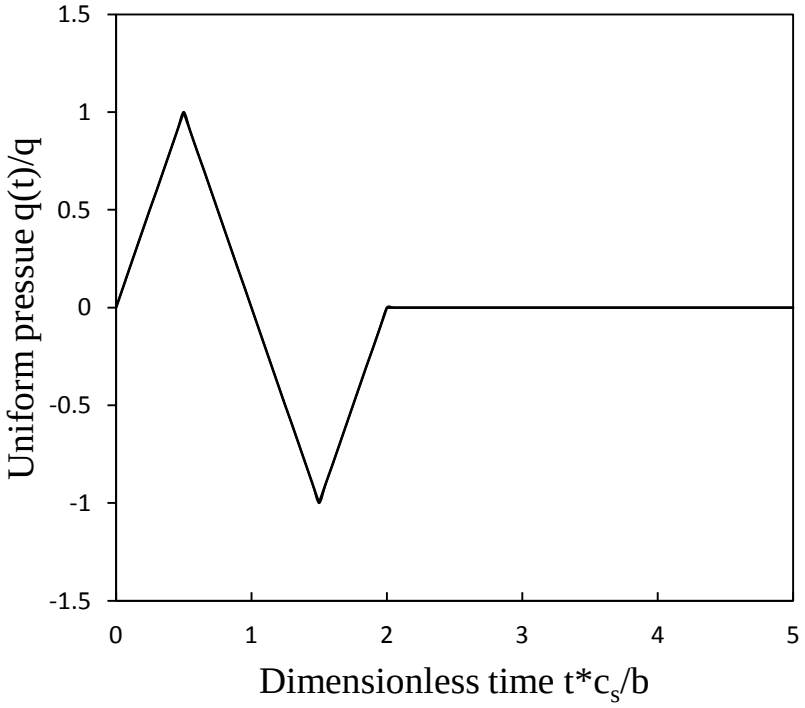

Figure 5. Time variation of uniformly distributed triangular pulse applied on top of the foundation

In order to verify the results, an extended mesh is analyzed using the finite element method. Figure 6 shows the meshing of the near field. Except in the region near the trench corner, eight-node isoparametric elements are used with the length and width equals to $0.1b$. In the region near the trench corner, due to stress concentration, a finer mesh is used. The far field up to the size of $80b \times 40e$ is also discretized using eight-node isoparametric elements. Due to the large size of the far field, the meshing is not shown in the figure. The extended mesh is chosen to be large enough so that for the time duration of $30b/c_s$, the dilatational wave generated by $p(t)$ does not reach its boundary. This extended finite element mesh results in 324713 elements

The dimensionless time step size for calculating the displacement unit-impulse response matrix is chosen as $\Delta t' = \Delta t c_s/b = 0.05$, while the time step size for the time domain analysis is $0.01b/c_s$. Therefore, 4 linear interpolation values need to be calculated within each time interval of the displacement unit-impulse response matrix. The vertical displacement u_{y1} in Figure 4 is calculated, first without truncation time, and then two different dimensionless truncation times $T' = Tc_s/b = 0.2$ or 0.1 are introduced. The results are plotted in Figure 7.

Figure 7 shows excellent agreement between the results obtained using the proposed method without truncation (full convolution) and the extended mesh. When a truncation time is introduced, the difference between the results with and without the truncation time is very small. Figure 8 shows the total CPU time (Intel i5-2500 @ 3.3 GHz, 8GB RAM) required for the computation up to a given dimensionless time. The original constant scheme is also used here as a comparison. It shows, the CPU time for the original method increases quadratically, since the total computational effort is proportional to n^2, where n is the number of time steps. For the new method without truncation, as a larger time step size is used for computing the displacement unit-impulse response matrix, the CPU time has been reduced significantly, although a quadratic increase is still observed. After the truncation time is introduced, the CPU time increases linearly, leading to a large saving of

computational cost (as at $t = 50b/c_s$, the CPU time is reduced to only 2% of that of the original method).

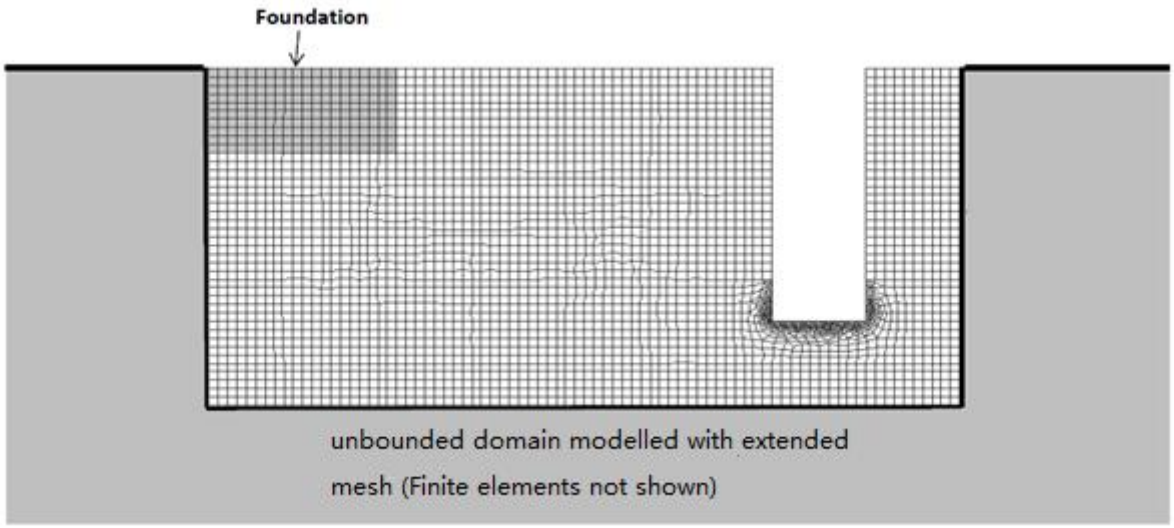

Figure 6. Finite element mesh of the near field

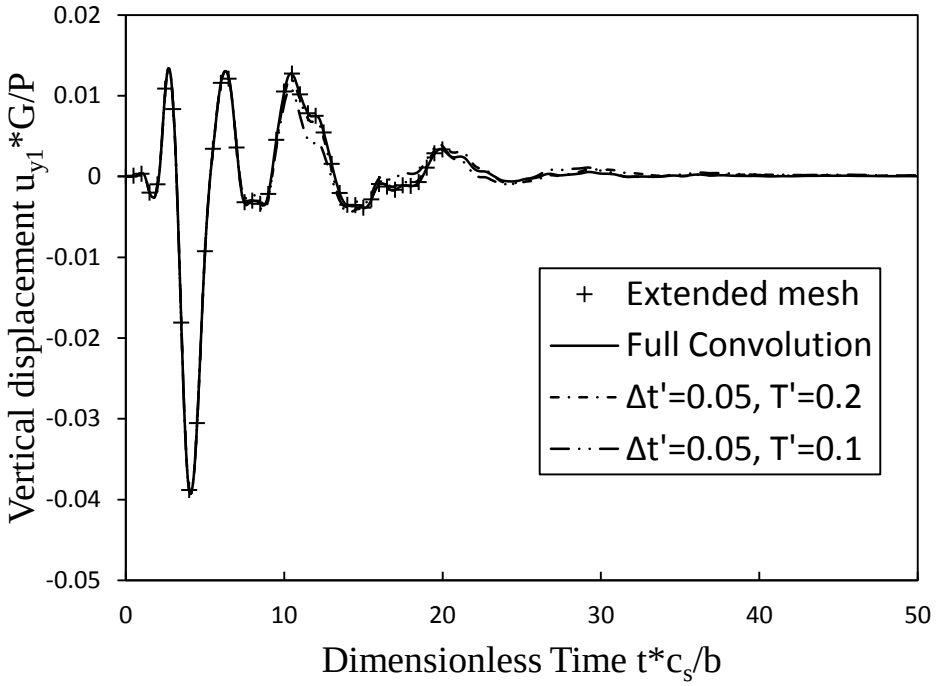

Figure 7. Normalized vertical displacement response u_{y1}

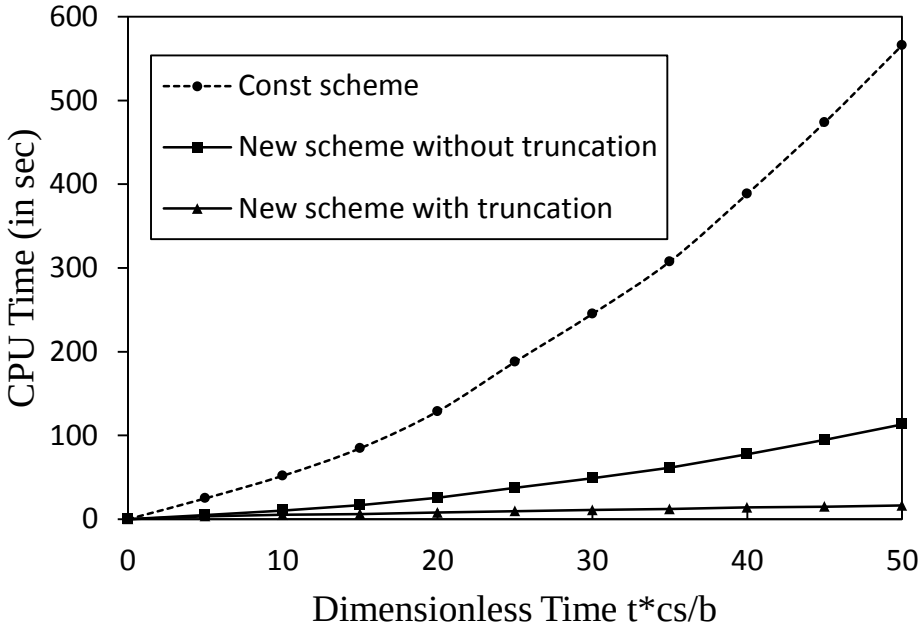

Figure 8. CPU time required for the computation

5. Conclusion

A new algorithm is developed which will be useful for the solution of dynamic soil-structure interaction problems in the time domain. The traditional SBFEM is based on approximating the acceleration unit-impulse response by a piece-wise constant function. Two essential improvements are proposed: (1) the displacement unit-impulse response is calculated instead of the acceleration unit-impulse response based on a piece-wise linear approximation; (2) the convolution integral in the soil-structure interaction force vector is truncated after a few steps. This leads to a significant reduction of computational effort. The accuracy and computational efficiency of the proposed algorithm have been verified by numerical examples. A wider range of applications of the new algorithm will be addressed in the near future.

Reference

Beskos, D. (1987). Boundary element methods in dynamic analysis. *Applied Mechanics Review*, 40,1-23.

Beskos, D. (1997). Boundary elements methods in dynamic analysis: Part II. *Applied Mechanics Review*, 50,149-197.

Bettess, P. (1992). *Infinite elements.* Sunderland: Penshaw Press.

Givoli, D. (1999). Exact representations on artificial interfaces and applications in mechanics. *Applied Mechanics Reviews*, 52(22), 333-349.

Radmanovic, B., & Katz, K. (2010). A high performance scaled boundary finite element method. *IOP Conf. Series: Materials Science and Engineering 10.*

Song, C. (2009). The scaled boundary finite element in structural dynamics. *International Journal for Numerical Methods in Engineering*, 77,1139-1171.

Tsynkov, S. (1998). Numerical solution of problems on unbounded domains: a review. *Applied Numerical Mathematics*, 27,465-532.

Wolf, J. (2003). *The Scaled Boundary Finite Element Method.* John Wiley & Sons.

Wolf, J., & Song, C. (1997). *Finite Element Modelling of Unbounded Media.* John Wiley & Sons.

Wolf, J., & Song, C. (1998). Unit-impulse response of unbounded medium by scaled boundary finite element method. *Computer Methods in Applied Mechanics and Engineering*, 159,355-367.